Electronic Supplementary Information for Dalton Transactions

Hydrogen Bonding in Schiff Bases – NMR, structural and experimental charge density studies

Anna Makal[1], Wojciech Schilf[2], Bohdan Kamieński[2,3], Anna Szady-Chelmieniecka[4], Eugeniusz Grech[4], Krzysztof Woźniak[1]*

[1]*Department of Chemistry, University of Warsaw, Pasteura 1,02-093 Warszawa, Poland*
[2]*Institute of Organic Chemistry, Polish Academy of Science, Kasprzaka 44/52, 01-224 Warszawa, Poland*
[3]*Institute of Physical Chemistry, Polish Academy of Science, Kasprzaka 44/52, 01-224 Warszawa, Poland*
[4]*Department of Inorganic and Analytical Chemisity West Pomeranian University of Technology, al. Piastów 42, 71-065 Szczecin, Poland*

Keywords: Schiff bases, NMR and solid state NMR, X-ray structure, experimental charge density, hydrogen bonding

Experimental

Synthesis of compounds. All compounds were synthesised by direct condensation of equimolar amount of amine and appropriate aldehyde in methanol solution at room temperature. For some systems a few hours of refluxing were necessary. The obtained Schiff bases were recrystalized from methanol. The yields of synthesis were from 65% for 2-hydroksy-5-nitrobenzaldehyde with 2-hydroksybenzyloamine to 85% for 2-hydroksybenzaladehyde with 2-aminophenole.

NMR Measurements. All NMR measurements in solution were performed on a Bruker Avance DRX 500 spectrometer operating at 500.13, 125.77 and 50.68 MHz for proton, carbon and nitrogen, respectively. For those experiments the 5 mm inverse, variable temperature PFG probe was used. Internal TMS and external nitromethane were used as the references for proton, carbon and nitrogen spectra, respectively. The assignment of the chemical shifts for carbon and nitrogen signals in solution was made by GHMBC and GHSQC methods. The standard Bruker procedures were used for acquisition and processing of data. The error in the chemical shift values was estimated to be 0.01 and 0.1 ppm for proton, carbon and nitrogen spectra, respectively.

The CPMAS spectra were run on Bruker Avance II 500 MHz instrument using a 4 mm probehead. The typical acquisition parameters for the natural abundance ^{15}N spectra were: spectral width 28 kHz, acquisition time 40 ms, spin rate 6-12 kHz, contact time for spin lock 5 ms and relaxation delay 10-120 s depending on the relaxation properties of a particular sample. The acquisition conditions for the ^{13}C CPMAS spectra were the following: spectral width 31 kHz, acquisition time 20 ms, contact time 2 ms and spin rate 12 kHz. The solid state spectra were originally referenced to the glycine sample and then the chemical shifts were recalculated to the TMS scale (for carbon) and nitromethane (for nitrogen). The signal assignment in the solid state ^{13}C spectra was made on the basis of a comparison with the liquid state spectra and by analysis of the short contact time spectra (SCT CPMAS), in this experiment only the signals from protonated carbon atoms are observed.

X-ray data collection. The data for compounds **VII**, **XV** and **XVI** were collected using the BRUKER KAPPA APEXII ULTRA controlled by APEXII software, equipped with MoKα rotating anode X-ray source (λ = 0.71073 A, 50.0 kV, 22.0 mA) monochromatized by multi-layer optics and APEX-II CCD detector. The experiments were carried out at 100K using the Oxford Cryostream cooling device. In the case of compounds **XV** and **XVI**, data

collection was also performed at room temperature. The crystals were mounted on thin cactus needle with a droplet of Paratone-N oil and immediately cooled. Indexing, integration and initial scaling were performed with *SAINT* and *SADABS* software [1]. The multi-scan absorption correction model was applied in the scaling procedure of **VII** and **XV**, while numeric absorption correction based on face indexing was emplyoyed for compound **XVI**. The data collection and processing statistics are reported in **Table 2** for according structures at appropriate temperatures. Additional high resolution X-ray data set was collected at 90K for compound **XV** in order to perform experimental charge density analysis. A total of 6265 frames of 0.5° oscillation width, divided into 34 omega scans, were collected. The generator settings were 50kV and 22mA and the crystal to detector distance was set to 50mm. The exposure time per frame varied with the detector position in 2θ angle as follows: 3s for 2.5°, 7.5°, ±10° and 20°, 5s for ±35° and -37.5°, 10s for -47.5°, 15s for ±52.5° and 57.5° and 25s for above ± 60°.

The unit cell parameters were obtained and refined based on the whole dataset. The average mosaicity was refined to the value of 0.6°. No decay of the samples during the measurements was observed. Finally the dataset was merged with SORTAV [2].

Conventional structure solution and refinement. The structures were solved by direct methods approach using the SHELXS-97 program and refined with the SHELXL-97 [3], as implemented in WinGX package [4]. The refinement was based on F^2 for all reflections except those with negative intensities. Weighted R factors wR and all goodness-of-fit S values were based on F^2, whereas conventional R factors were based on the amplitudes, with F set to zero for negative F^2. The $F_0^2 > 2\sigma(F_0^2)$ criterion was applied only for R factors calculation was not relevant to the choice of reflections for the refinement. The R factors based on F^2 are for all structures about twice as large as those based on F. The hydrogen atoms were initially located from the Fourier map. Than the hydrogen atoms which did not participate in strong hydrogen bonds were moved to idealised geometrical positions, and their temperature displacement parameters were refined isotropically as a riding on the connected carbon atoms. Isotropic thermal displacement parameters for hydrogen atoms involved in hydrogen bonds were left to refine without constraints, in order to measure to what degree the electron density of these atoms is diffused. Scattering factors were taken from Tables 4.2.6.8 and 6.1.1.4 from the International Crystallographic Tables Vol. C. [5] Details of the data collection and refinement are presented in **Table 2**.

Experimental charge density analysis. The program *XDLSM* of the package *XD* [6] was used for the purpose of multipole refinement. The Hansen-Coppens formalism [7] , was applied. In this model electron density in the crystal is assumed to consist of the sum of atomic contributions centered at the atomic positions. The atomic electron density is divided into three components:

$$\rho_k(r_k) = \rho_{core}(r_k) + P_{valence}\kappa^3\rho_{valence}(\kappa r_k) + \kappa'^3\sum_{l=0}^{l_{max}} R_l(\kappa' r_k)\sum_{m=-l}^{+l} P_{lm\pm} d_{lm\pm}(\ _k,\ _k)$$

(a) a spherically averaged free-atom Hartree-Fock core contribution, ρ_{core}; (b) a spherically averaged free-atom Hartree-Fock normalized to one electron valence contribution, $\rho_{valence}$, with refineble population parameter $P_{valence}$ and the dimensionless expansion-contraction parameter κ; and (c) a deformation term expressed as normalized Slater-type radial function $R_l(\mathbf{r}_k)$ modulated by density normalized, real spherical harmonic angular functions $d_{lm\pm}(\vartheta,\varphi)$ defined on local axes centered on the atoms and with population parameters $P_{lm\pm}$. representing the deviation of the valence density from spherical symmetry, modified by the dimensionless expansion-contraction parameter κ'. Scattering factors for all atoms were derived from wave functions tabulated by Clementi & Roetti [8]. Local coordinate systems were defined for all atoms in a way that enabled application of symmetry constraints in the later stages of refinement. The ring C atoms were expected to obey local m symmetry where m would be the

plane of benzene ring, with z-axis perpendicular to it. The carbons in methyl groups were to obey 3m symmetry with 3-fold axis (z-axis) located along C-C bond.

The refinement with XDLSM of positional and thermal parameters of non-hydrogen atoms against a whole dataset with statistical weighting scheme was conducted for each of the three datasets. After it had reached convergence we inspected difference density maps. Well pronounced residuals indicating highly aspherical electron density distribution in the regions of bonds were observed.

In the lack of neutron data, which would be the most precise source of information on the hydrogen atoms positions and thermal motion, the anisotropic thermal displacement parameters for all hydrogen atoms in **XV** were estimated using SHADE2 [9] server. Detailed procedure was conducted according to the paper by Hoser et.al [10]. The use of simulated ADP-s for hydrogens have already been shown to significantly improve the results of experimental charge density refinements [11]. Estimated ADP-s for hydrogens were incorporated into a model and kept fixed during the proceeding multipole refinements.

The remaining positional and thermal parameters were also fixed at the next refinement stage. Local symmetry constraints were applied to the multipole populations of selected atoms according to their closest environments. Chemical constraints were applied to H atoms: hydrogens belonging to the same benzene ring or methyl group were forced to have similar multipolar populations. The multipole refinements were conducted in stepwise manner, up to the hexadecapole level for non-H atoms, bond directed dipoles and quadrupoles for hydrogens. When the multipole populations converged, the kappa parameters were let to refine. At last the positional and thermal parameters of non-H atoms were refined with the multipole populations fixed. All the refinements converged satisfactorily, with max shift to standard deviation ratio going well below 10^{-7}. The summary of the refinements results for all three compounds is presented in **Table 2**. The residual density values are below +/- 0.15 e $Å^{-3}$ and the residual map is featureless according to visual inspection and featurelessness tests made with jnk2RDA program [12] (Figure **1S** in **the Supporting Materials**). The fractal dimension plot is reported in the Supporting Materials together with the residual density map. The normal probability plot [13] was also examined, proving satisfactory fit of the model to the experimental data. The Hirshfeld test [14] gives the average value of 2, and the highest observed value is 5 in the case of N1-C9 formally single bond. This suggests that the refinements were complete and atomic thermal motions well resolved in the case of all compounds.

The topological analysis of the charge density ρ(r) and laplacian Lap(r) were conducted with XDPROP program of XD package [6] in accordance with the Bader's theory of Atoms in Molecules (AIM) [15]. The kinetic energy densities $G(r_{BCP})$ at bond critical points (BCP) were estimated using the approximation of Abramov [16], $G(r_{BCP}) = 0.3\left(\frac{3\pi}{2}\right)^{\frac{2}{3}} \rho(r_{BCP})^{\frac{5}{3}} + \frac{1}{6} L(r_{BCP})$, while the corresponding potential energy densities at BCP $V(r_{BCP})$ were obtained from the local virial theorem: $V(r_{BCP}) = \frac{1}{4} L(r_{BCP}) - 2G(r_{BCP})$, and the total energy density at BCP was estimated as $H(r_{BCP}) = G(r_{BCP}) + V(r_{BCP})$.

Table 1S. Data collection, structure solution and refinement details for compounds **VII**, **XV** and **XVI**.

	VII	**XV**	**XV**	**XV**	**XVI**	**XVI**
Temperature [K]	**100**	**100**	**90**	**298**	**100**	**298**

Formula	$C_{14}H_{13}NO_3$	$C_{15}H_{15}NO_3$	$C_{15}H_{15}NO_3$	$C_{15}H_{15}NO_3$	$C_{14}H_{12}BrNO_2$	$C_{14}H_{12}BrNO_2$
Weight	243.25	257.28	257.28	257.28	306.16	306.16
System	monoclinic	monoclinic	monoclinic	monoclinic	monoclinic	monoclinic
Space group	P2(1)/c	P2(1)/c	P2(1)/c	P2(1)/c	C2/c	C2/c
a [Å]	9.6676(5)	6.9584(3)	6.9521(2)	7.1443(3)	21.8260(18)	21.8167(15)
b [Å]	9.2734(4)	9.4535(3)	9.4671(3)	9.5579(4)	5.3467(4)	5.4273(5)
c [Å]	12.5025(5)	19.2626(8)	19.2841(6)	19.0902(7)	21.9362(18)	22.1970(14)
α [°]	90.00	90.00	90.00	90.00	90.00	90.00
β [°]	93.359(3)	95.819(2)	95.7990(10)	95.868(2)	103.650(2)	103.351(2)
γ [°]	90.00	90.00	90.00	90.00	90.00	90.00
V [$Å^3$]	1118.94(9)	1260.59(9)	1262.71(7)	1296.73(9)	2487.6(3)	2557.2(3)
Z	4	4	4	4	8	8
Shape	planar	prismatic	prismatic	prismatic	planar	planar
Color	red	orange	orange	orange	yellow	yellow
Size max. [mm]	0.21	0.18	0.18	0.36	0.26	0.36
Size mid. [mm]	0.11	0.17	0.17	0.22	0.11	0.21
Size min. [mm]	0.03	0.11	0.11	0.15	0.03	0.05
Density [g/cm^3]	1.444	1.356	1.353	1.356	1.635	1.590
F000	512	544	544	544	1232	1232
μ [mm^{-1}]	0.102	0.095	0.095	0.095	3.297	3.297
Tmin /Tmax					0.654 / 0.906	0.456 / 0.851
Rint	0.0313	0.0244	0.0351	0.0190	0.0302	0.0318
sinθ/λ [$Å^{-1}$]	0.65	0.68	1.17	0.68	0.67	0.65
Completeness [%]	99.9	99.5	95.3	99.6	99.6	96.6
N.refl	2562	3129	16105	3305	3066	2825
N.refl >2σ	2083	2524	10969	2302	2657	2006
			REFINEMENT			
N.par	215	232	232	232	211	211
R(F)	0.0376	0.0383	0.0403	0.0423	0.0258	0.0363
R(F)all	0.0502	0.0506	0.0631	0.0663	0.0332	0.0625
wR2	0.0922	0.0990	0.1266	0.1022	0.0646	0.0874
GooF	1.019	1.060	1.118	1.026	1.034	1.042
Highest peak	0.289	0.361	0.696	0.164	0.768	0.449
Deepest hole	-0.221	-0.210	-0.271	-0.177	-0.316	-0.292
RMS [e $Å^{-3}$]	0.047	0.043	0.074	0.032	0.070	0.058
			MULTIPOLE REFINEMENT			
N.par			551			
Nref / Npar			16.8			
R(F)			0.018			
R(F)all			0.047			
wR2			0.023			
GooF			1.589			
Highest peak			0.133			
Deepest hole			-0.098			
RMS [e $Å^{-3}$]			0.028			

Table 2S. More important parameters of experimental charge density at bond critical points in compound **XV**. Symmetry operation X3: 1 - X, 2 - Y, - Z

Bond	$\rho(r_{BCP})$ [eÅ^{-3}]	$\nabla^2(r_{BCP})$ [eÅ^{-5}]	$G(r_{BCP})$ [Ha$_0^{-3}$]	$V(r_{BCP})$ [Ha$_0^{-3}$]	$H(r_{BCP})$ [Ha$_0^{-3}$]	$G(r_{BCP})$ /$\rho(r_{BCP})$ [H/e]	$H(r_{BCP})$ /$\rho(r_{BCP})$ [H/e]	$\lvert V(r_{BCP})\rvert$/ $G(r_{BCP})$
O(1)-H(1N)	0.264(10)	3.334(10)	0.04	-0.04	0	0.92	-0.03	1.03
O(1)-X3_H(3O)	0.467(37)	2.326(68)	0.05	-0.08	-0.03	0.72	-0.36	1.5
O(3)-H(1N)	0.066(5)	1.341(2)	0.01	-0.01	0	1.13	0.31	0.64
O(1)-C(2)	2.596(15)	-27.153(77)	0.4	-1.08	-0.68	1.03	-1.76	2.71
O(2)-C(5)	2.211(13)	-18.707(60)	0.32	-0.83	-0.51	0.97	-1.56	2.61
O(2)-C(7)	1.891(15)	-14.586(60)	0.24	-0.64	-0.4	0.87	-1.41	2.62
O(3)-C(11)	2.286(14)	-21.376(68)	0.33	-0.87	-0.55	0.96	-1.62	2.68
O(3)-H(3O)	2.59(1)	-48.55(1)	0.246	-0.995	-0.749	0.64	-1.95	4.04
N(1)-H(1N)	2.816(51)	-38.566(407)	0.4	-1.21	-0.8	0.96	-1.92	3
N(1)-C(8)	2.687(17)	-28.866(69)	0.42	-1.14	-0.72	1.05	-1.81	2.72
N(1)-C(9)	1.805(14)	-11.351(48)	0.24	-0.6	-0.36	0.9	-1.34	2.49
C(1)-C(2)	2.081(12)	-17.247(37)	0.29	-0.75	-0.46	0.92	-1.51	2.63
C(1)-C(6)	2.088(12)	-16.569(36)	0.29	-0.76	-0.46	0.94	-1.5	2.59
C(1)-C(8)	2.136(12)	-18.135(38)	0.3	-0.78	-0.49	0.94	-1.53	2.63
C(2)-C(3)	2.102(12)	-17.389(37)	0.29	-0.76	-0.47	0.93	-1.51	2.62
C(3)-C(4)	2.313(14)	-20.489(40)	0.34	-0.89	-0.55	0.99	-1.61	2.63
C(3)-H(3)	2.036(39)	-21.672(122)	0.24	-0.7	-0.47	0.8	-1.54	2.93
C(4)-C(5)	2.144(12)	-18.932(38)	0.29	-0.78	-0.49	0.93	-1.54	2.67
C(4)-H(4)	2.004(38)	-21.347(129)	0.23	-0.69	-0.45	0.78	-1.53	2.95
C(5)-C(6)	2.283(13)	-20.453(40)	0.33	-0.87	-0.54	0.98	-1.6	2.65
C(6)-H(6)	2.000(39)	-21.510(139)	0.23	-0.68	-0.45	0.78	-1.53	2.97
C(7)-H(7A)	1.955(25)	-17.845(72)	0.24	-0.67	-0.43	0.83	-1.47	2.77
C(7)-H(7B)	1.955(4)	-17.748(14)	0.24	-0.67	-0.43	0.83	-1.47	2.77
C(7)-H(7C)	1.948(4)	-17.688(13)	0.24	-0.66	-0.42	0.83	-1.47	2.76
C(8)-H(8)	1.997(36)	-21.035(136)	0.23	-0.68	-0.45	0.78	-1.52	2.94
C(9)-C(10)	1.768(11)	-11.803(33)	0.23	-0.58	-0.35	0.86	-1.33	2.54
C(9)-H(9A)	1.893(28)	-18.807(100)	0.22	-0.63	-0.41	0.77	-1.46	2.91
C(9)-H(9B)	1.929(12)	-19.441(39)	0.22	-0.65	-0.42	0.78	-1.48	2.91
C(10)-C(11)	2.233(12)	-20.687(39)	0.31	-0.84	-0.53	0.94	-1.59	2.69
C(10)-C(15)	2.161(14)	-16.338(40)	0.32	-0.8	-0.49	0.99	-1.52	2.54
C(11)-C(12)	2.247(13)	-19.801(40)	0.32	-0.85	-0.53	0.97	-1.59	2.64
C(12)-C(13)	2.241(14)	-20.120(42)	0.32	-0.85	-0.53	0.96	-1.59	2.66
C(12)-H(12)	1.877(35)	-16.301(133)	0.23	-0.62	-0.4	0.82	-1.43	2.74
C(13)-C(14)	2.188(16)	-18.243(49)	0.31	-0.82	-0.5	0.97	-1.55	2.61
C(13)-H(13)	1.831(35)	-16.927(155)	0.21	-0.6	-0.39	0.77	-1.42	2.85
C(14)-C(15)	2.180(15)	-18.469(50)	0.31	-0.81	-0.5	0.96	-1.55	2.62
C(14)-H(14)	1.907(42)	-17.458(161)	0.23	-0.64	-0.41	0.81	-1.45	2.79
C(15)-H(15)	1.981(39)	-19.191(135)	0.24	-0.68	-0.44	0.82	-1.5	2.83

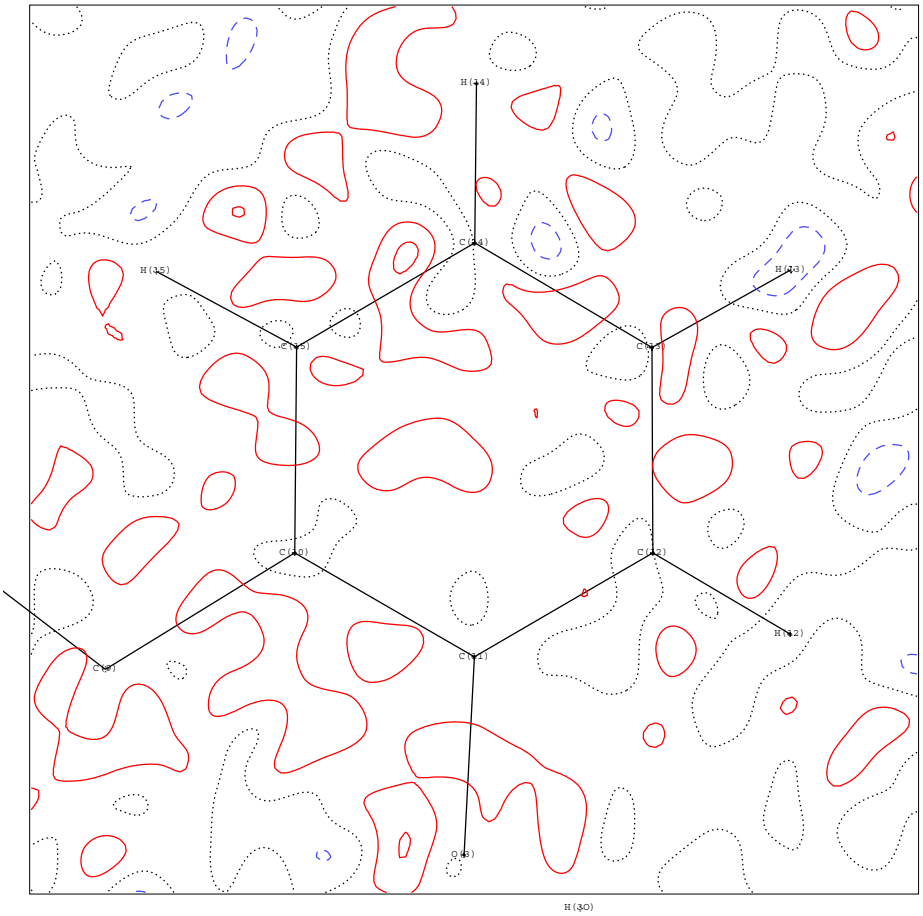

Figure 1S. Residual density map for the final multipole model of charge density of **XV**.

Table 3S. Definition of the selected atomic parameters obtained in multipolar refinement.

	Pval	Kappa	Kappa'	Monopole charge	AIM charge
O(1)	6.533(18)	0.987(1)	0.937(24)	-0.532(18)	-1.096
O(2)	6.344(18)	0.987(1)	0.937(24)	-0.343(18)	-1.033
O(3)	6.430(24)	0.987(1)	0.937(24)	-0.429(24)	-1.094
N(1)	5.014(52)	1.014(3)	0.991(43)	-0.013(52)	-0.919
C(1)	4.081(26)	1.025(2)	0.890(5)	-0.081(26)	-0.098
C(2)	4.059(25)	1.025(2)	0.890(5)	-0.059(25)	0.501
C(3)	3.993(33)	1.025(2)	0.890(5)	0.007(33)	0.015
C(4)	3.994(32)	1.025(2)	0.890(5)	0.005(32)	0.004
C(5)	4.008(26)	1.025(2)	0.890(5)	-0.007(26)	0.415
C(6)	3.938(32)	1.025(2)	0.890(5)	0.062(32)	0.060
C(7)	3.509(40)	1.025(2)	0.890(5)	0.490(40)	0.710
C(8)	4.065(32)	1.025(2)	0.890(5)	-0.064(32)	0.469
C(9)	3.964(36)	1.025(2)	0.890(5)	0.036(36)	0.316
C(10)	4.094(28)	1.025(2)	0.890(5)	-0.094(28)	-0.104
C(11)	4.005(27)	1.025(2)	0.890(5)	-0.004(27)	0.437
C(12)	4.103(32)	1.025(2)	0.890(5)	-0.102(32)	-0.093
C(13)	4.173(36)	1.025(2)	0.890(5)	-0.173(36)	-0.113
C(14)	4.129(39)	1.025(2)	0.890(5)	-0.129(39)	-0.066
C(15)	3.857(36)	1.025(2)	0.890(5)	0.142(36)	0.125
H(3)	1.019(21)	1.235(8)	1.200	-0.018(21)	-0.029
H(4)	0.930(20)	1.235(8)	1.200	0.069(20)	0.061
H(6)	0.911(20)	1.235(8)	1.200	0.089(20)	0.075
H(7A)	1.048(13)	1.235(8)	1.200	-0.047(13)	-0.021
H(7B)	1.048	1.235(8)	1.200	-0.04770	-0.021
H(7C)	1.048	1.235(8)	1.200	-0.04770	-0.018
H(8)	0.896(19)	1.235(8)	1.200	0.104(19)	0.069
H(9A)	0.872(15)	1.235(8)	1.200	0.128(15)	0.097
H(9B)	0.872	1.235(8)	1.200	0.12800	0.099
H(12)	0.886(20)	1.235(8)	1.200	0.114(20)	0.091
H(13)	0.769(19)	1.235(8)	1.200	0.230(19)	0.187
H(14)	0.871(21)	1.235(8)	1.200	0.129(21)	0.064
H(15)	0.954(22)	1.235(8)	1.200	0.046(22)	0.044
H(1N)	0.913(25)	1.235(8)	1.200	0.087(25)	0.301
H(3O)	0.729(17)	1.235(8)	1.200	0.271(17)	0.505

Table 4S. More important structural parameters for compound **VII, XV** and **XVI** (distances in Å, angles and torsions in °)

VII

Parameter	value
O(1)-C(1)	1.3102(16)
O(3)-C(10)	1.3479(16)
O(3)-H(3O)	0.93(2)
N(1)-C(8)	1.2997(17)
N(1)-C(9)	1.4107(17)
N(1)-H(1N)	0.924(18)
C(1)-C(2)	1.4071(19)
C(1)-C(6)	1.4316(18)
C(2)-C(3)	1.3773(19)
C(3)-C(4)	1.4026(19)
C(4)-C(5)	1.3761(19)
C(5)-C(6)	1.4103(18)
C(6)-C(8)	1.4227(18)
C(9)-C(14)	1.3913(18)
C(9)-C(10)	1.4042(18)
C(10)-C(11)	1.3928(18)
C(11)-C(12)	1.3869(19)
C(12)-C(13)	1.3875(19)
C(13)-C(14)	1.3842(19)
C(10)-O(3)-H(3O)	109.3(13)
C(8)-N(1)-C(9)	127.37(11)
C(8)-N(1)-H(1N)	114.6(11)
C(9)-N(1)-H(1N)	118.0(11)
O(1)-C(1)-C(6)	121.42(12)
C(8)-C(6)-C(1)	120.37(12)
N(1)-C(8)-C(6)	121.41(12)
C(10)-C(9)-N(1)	116.20(11)
O(3)-C(10)-C(11)	122.93(12)
O(3)-C(10)-C(9)	118.18(12)
O(1)-C(1)-C(2)-C(3)	179.91(13)
C(7)-O(2)-C(4)-C(3)	6.7(2)
C(2)-C(1)-C(6)-C(8)	-178.74(12)
C(9)-N(1)-C(8)-C(6)	179.10(12)
C(1)-C(6)-C(8)-N(1)	2.35(19)
C(8)-N(1)-C(9)-C(14)	14.1(2)
N(1)-C(9)-C(10)-O(3)	2.09(17)
O(3)-C(10)-C(11)-C(12)	178.88(12)

XV

O(1)	C(2)	1.2979(3)
O(2)	C(5)	1.3649(3)
O(2)	C(7)	1.4213(4)
O(3)	C(11)	1.3440(3)
O(3)	H(3O)	0.8823(3)
N(1)	C(8)	1.3025(3)
N(1)	C(9)	1.4631(3)
N(1)	H(1N)	0.8784(2)
C(1)	C(2)	1.4284(3)
C(1)	C(6)	1.4204(3)
C(1)	C(8)	1.4190(3)
C(2)	C(3)	1.4264(3)
C(3)	C(4)	1.3759(3)
C(3)	H(3)	1.0800(2)
C(4)	C(5)	1.4129(3)
C(4)	H(4)	1.0800(2)
C(5)	C(6)	1.3751(3)
C(6)	H(6)	1.0800(2)
C(7)	H(7A)	1.0600(2)
C(7)	H(7B)	1.0600(2)

C(7) - H(7C)	1.06000(19)	
C(8) - H(8)	1.0800(2)	
C(9) - C(10)	1.5057(3)	
C(9) - H(9A)	1.0900(2)	
C(9) - H(9B)	1.0900(2)	
C(10) - C(11)	1.4057(3)	
C(10) - C(15)	1.3940(3)	
C(11) - C(12)	1.3987(3)	
C(12) - C(13)	1.3911(3)	
C(12) - H(12)	1.0800(3)	
C(13) - C(14)	1.3940(4)	
C(13) - H(13)	1.0800(3)	
C(14) - C(15)	1.3980(4)	
C(14) - H(14)	1.0800(3)	
C(15) - H(15)	1.0800(3)	

C(5) - O(2) - C(7)	116.65(2)		
C(11) - O(3) - H(3O)	111.40(2)		
C(8) - N(1) - C(9)	123.78(2)		
C(8) - N(1) - H(1N)	115.36(2)		
C(9) - N(1) - H(1N)	120.83(2)		
C(2) - C(1) - C(6)	121.584(19)		
C(2) - C(1) - C(8)	120.553(18)		
C(6) - C(1) - C(8)	117.862(18)		
O(1) - C(2) - C(1)	121.37(2)		
O(1) - C(2) - C(3)	122.31(2)		
C(1) - C(2) - C(3)	116.320(18)		
C(2) - C(3) - C(4)	121.17(2)		
C(2) - C(3) - H(3)	118.087(19)		
C(4) - C(3) - H(3)	120.74(2)		
C(3) - C(4) - C(5)	121.75(2)		
C(3) - C(4) - H(4)	120.83(2)		
C(5) - C(4) - H(4)	117.421(19)		
O(2) - C(5) - C(4)	114.87(2)		
O(2) - C(5) - C(6)	126.04(2)		
C(4) - C(5) - C(6)	119.088(19)		
C(1) - C(6) - C(5)	120.065(19)		
C(1) - C(6) - H(6)	118.139(19)		
C(5) - C(6) - H(6)	121.795(19)		
O(2) - C(7) - H(7A)	110.689(19)		
O(2) - C(7) - H(7B)	111.242(19)		
O(2) - C(7) - H(7C)	105.52(2)		
H(7A) - C(7) - H(7B)	109.58(2)		
H(7A) - C(7) - H(7C)	110.314(18)		
H(7B) - C(7) - H(7C)	109.427(18)		
N(1) - C(8) - C(1)	123.73(2)		
N(1) - C(8) - H(8)	117.21(2)		
C(1) - C(8) - H(8)	119.058(18)		
N(1) - C(9) - C(10)	111.211(17)		
N(1) - C(9) - H(9A)	107.18(2)		
N(1) - C(9) - H(9B)	108.646(18)		
C(10) - C(9) - H(9A)	110.868(17)		
C(10) - C(9) - H(9B)	110.84(2)		
H(9A) - C(9) - H(9B)	107.954(18)		
C(9) - C(10) - C(11)	118.362(19)		
C(9) - C(10) - C(15)	122.10(2)		
C(11) - C(10) - C(15)	119.50(2)		
O(3) - C(11) - C(10)	117.05(2)		
O(3) - C(11) - C(12)	123.18(2)		
C(10) - C(11) - C(12)	119.77(2)		
C(11) - C(12) - C(13)	119.94(2)		
C(11) - C(12) - H(12)	119.22(2)		

C(13) - C(12) - H(12)	120.83(2)
C(12) - C(13) - C(14)	120.84(3)
C(12) - C(13) - H(13)	118.94(3)
C(14) - C(13) - H(13)	120.21(3)
C(13) - C(14) - C(15)	119.09(2)
C(13) - C(14) - H(14)	119.95(3)
C(15) - C(14) - H(14)	120.96(3)
C(10) - C(15) - C(14)	120.86(3)
C(10) - C(15) - H(15)	117.80(3)
C(14) - C(15) - H(15)	121.33(2)

XVI

Br(1)-C(4)	1.9005(19)	1.898(3)
O(1)-C(1)	1.289(2)	1.290(3)
O(2)-C(10)	1.355(2)	1.354(3)
O(2)-H(2O)	0.86(3)	0.81(4)
N(1)-C(7)	1.284(3)	1.271(4)
N(1)-C(8)	1.470(2)	1.473(4)
N(1)-H(1N)	0.81(2)	0.83(3)
C(1)-C(2)	1.420(3)	1.413(4)
C(1)-C(6)	1.439(2)	1.427(4)
C(2)-C(3)	1.373(3)	1.380(4)
C(3)-C(4)	1.407(3)	1.394(4)
C(4)-C(5)	1.365(3)	1.366(4)
C(5)-C(6)	1.407(3)	1.406(4)
C(6)-C(7)	1.422(3)	1.426(4)
C(8)-C(9)	1.502(3)	1.491(4)
C(9)-C(14)	1.389(3)	1.391(4)
C(9)-C(10)	1.401(3)	1.396(4)
C(10)-C(11)	1.391(3)	1.377(4)
C(11)-C(12)	1.388(3)	1.386(5)
C(12)-C(13)	1.386(3)	1.363(6)
C(13)-C(14)	1.390(3)	1.382(5)
C(10)-O(2)-H(2O)	111(2)	113(3)
C(7)-N(1)-C(8)	125.23(15)	126.4(2)
C(7)-N(1)-H(1N)	113.1(18)	114(2)
C(8)-N(1)-H(1N)	121.6(18)	119(2)
O(1)-C(1)-C(6)	121.41(16)	121.5(2)
C(5)-C(4)-Br(1)	120.59(14)	120.6(2)
C(3)-C(4)-Br(1)	118.74(15)	119.0(2)
C(7)-C(6)-C(1)	120.31(17)	120.0(3)
N(1)-C(7)-C(6)	123.03(16)	123.7(2)
N(1)-C(8)-C(9)	109.67(14)	110.2(2)
C(10)-C(9)-C(8)	118.48(16)	119.1(2)
O(2)-C(10)-C(11)	123.77(17)	124.0(3)
O(2)-C(10)-C(9)	115.94(16)	115.5(2)
O(1)-C(1)-C(2)-C(3)	-179.85(17)	-179.6(3)
Br(1)-C(4)-C(5)-C(6)	-177.72(13)	-177.9(2)
O(1)-C(1)-C(6)-C(7)	1.6(3)	1.9(4)
C(8)-N(1)-C(7)-C(6)	179.68(16)	-179.7(2)
C(1)-C(6)-C(7)-N(1)	0.5(3)	-0.3(4)
C(7)-N(1)-C(8)-C(9)	128.33(18)	128.7(3)
N(1)-C(8)-C(9)-C(10)	69.3(2)	69.9(3)
C(8)-C(9)-C(10)-O(2)	-0.5(2)	-0.2(4)

Weak interactions. An infinite network of intra and intermolecular hydrogen bonds is formed in the crystal structure of **VII**. According to Etter hydrogen bond classification based on graph theory [17], the network is complex, including intramolecular set of hydrogen bonds S21(9), combined in an infinite chain C(5). The chain of molecules connected by intermolecular hydrogen bonds follows the [010] crystallographic direction, and molecules

participating in its formation are related by $2_{[010]}$ screw axis symmetry operation. The molecules constituting the chain are tilted nearly perpendicularly to each other. The interactions between the chains are based on stacking, taking place between the molecules belonging to the two neighbouring chains, and related by crystallographic centre of symmetry. The ring C1-C6 locates directly over the pseudo six membered ring including conjugated Schiff base fragment and intramolecular hydrogen bond: C1 locates directly over C6, O1 over C5 and N1 over C3, the closest distance between the planes of C1-C6 ring and the plane of Schiff-base fragment being 3.244(3) Å. Packing and the H-bond network for the compound **VII** is presented in the Figure 2S, whereas the details of H-bonds in Table 3.

Compounds **XV** and **XVI** represent the A' family of Schiff base derivatives. An additional methylene group divides the Schiff base fragment from the phenyl substituent, and introduces a bent into the molecules of **XV** and **XVI** compound. A measure of this bent may be the value of torsion around the N1-C9 bond (**XV**) or N1-C8 bond (**XVI**), reported in the Supporting Materials, respectively. In the case of the bromine substituted compound **XVI**, the rotation around the N1-C8 bond is by 10 degrees larger than the analogous rotation in **XV**. In both cases, the imine fragment is strictly coplanar with the C1-C6 ring.

A common packing motif can be observed for the two compounds. The molecules related by crystallographic centre of symmetry build dimers bound by hydrogen bonds. The whole H-bond network for **XV** and **XVI** can be classified as R22(10)S21(10) according to the Etter terminology.

The dimers form stacks of translation-related moieties along the [010] crystallographic direction in both **XV** and **XVI** compounds structure. However, different space groups and crystal packing between the compounds results from different substituents at the 4 position, and, therefore, different intermolecular interactions.

In the case of methoxy substituent, the methoxy oxygen atom belonging to one of the columns of dimers locates exactly in between two Schiff-base fragments belonging to the next column in the [100] direction. π…π stacking can be observed along the [100] direction, with the closest distance between the parallel fragments being 3.33(2)Å. In such a setting, there are possibilities for the H7A and H7B atoms to form weak hydrogen bonds with symmetry related O1 and O3 oxygens, respectively. Interactions between the neighbouring columns of dimers along the [001] directions are dominated by C-H…π interactions.

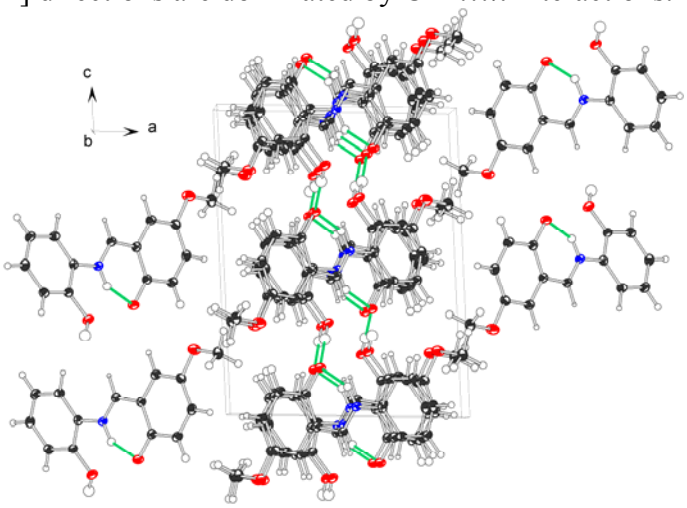

(a)

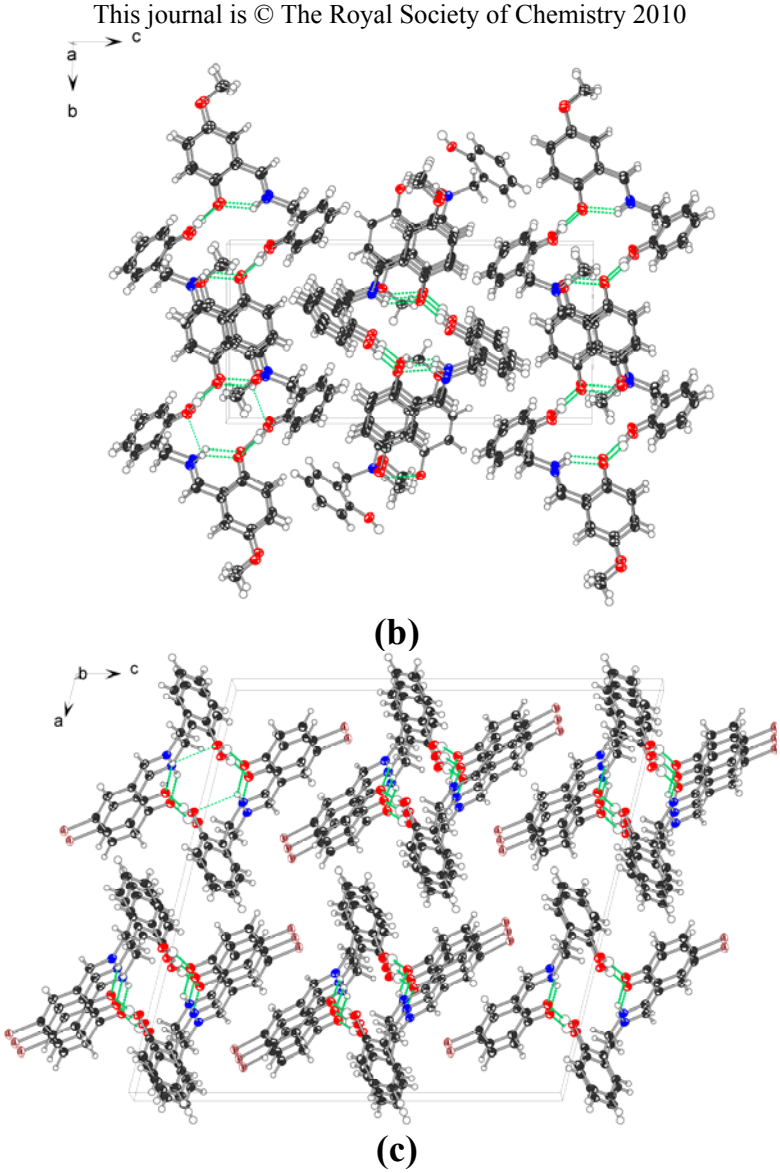

Figure 2S. Illustration of packing: (a) along [010] direction in the crystal structure of **VII** at 100K, (c) along [100] direction in the crystal structure of **XV**, (e) along [010] direction in the crystal structure of and **XVI**.

In the case of the bromine derivative, halogen substituents are located far from the Schiff-base fragments. The columns of hydrogen bonded dimers are well separated, and interactions between the columns are dominated by short C-H…Br contacts along the [001] direction – layers rich in Br are present, perpendicular to the [001] direction. In the [100] direction, the interactions between the neighbouring columns of dimers are dominated by C-H…π contacts.

There are no direct stacking interactions inside the column of dimers, although the shortest distance between the planes of two adjacent C1-C6 rings is as small as 2.94(3)Å. The dimers are shifted along the [010] with respect to one another in a way, that places the N1 atom from the second dimer as close as 3.06(4)A above the O2 atom from the original dimer.

References

[1] a) APEXII-2008v1.0 Bruker Nonius 2007, b) SAINT V7.34A Bruker Nonius 2007, c) SADABS-2004/1 Bruker Nonius area detector scaling and absorption correction, 2007
[2] R.H. Blessing, Acta Cryst., A51 (1995) 33-38
[3] G.M. Sheldrick, Acta Cryst., A64, (2008) 112-122.

[4] L. J. Farrugia, J. Appl. Cryst. **32** (1999) 837-838.
[5] *International Tables for Crystallography*, Ed. A. J. C. Wilson, Kluwer:Dordrecht, **1992**, Vol.C.
[6] A. Volkov, P. Macchi, L. J. Farrugia, C. Gatti, P. Mallinson, T. Richter, T. Koritsanszky, XD2006 – A computer program for multipole refinement, topological analysis of charge densities and evaluation of intermolecular energies form experimental or theoretical structure factors (2006).
[7] P. Coppens, *X-Ray Charge Densities and Chemical Bonding.* Oxford University Press, (1997).
[8] E. Clementi, C. Roetti, Atomic and Nuclear Data Tables, 14 (1974) 177.
[9] A. O. Madsen, J. Appl. Cryst., 39 (2006) 757-758.
[10] A. A. Hoser, P. M. Dominiak and K. Woźniak, Acta. Cryst., A65(4) (2009) 300-311.
[11] P. Munshi, A. O. Madsen, M. A. Spackman, S. Larsen, R. Destro, ActaCryst., A64, (2008) 465.
[12] Meindl, K., Henn, J., Acta Cryst., A64 (2008) 404–418.
[13] S. C. Abrahams, E. T. Keve, Acta Cryst. A27 (1971) 157-165.
[14] F. L. Hirshfeld, Acta Cryst., A32 (1976) 239-244.
[15] R. F. Bader, *Atoms in Molecules. A Quantum Theory*, Clarendon Press, Oxford, 1994.
[16] Y. A. Abramov. Acta Cryst., A53 (1997) 264.
[17] M. C. Etter and J. C. MacDonald and J. Bernstein, Acta Cryst. B, 46 (1990) 256-262.